Journal of Applied Polymer Science

Morphology and Antibacterial Properties of Natural Rubber Composites Based on Biosynthesized Nanosilver

Yongqiang Zhang, Xinghua Xue, Ziqi Zhang, Yafei Liu, Guang Li
College of Materials and Chemical Engineering, Hainan University, Haikou 570228, People's Republic of China
Correspondence to: X. Xue (E-mail: xxh408@163.com)

ABSTRACT: The objective of this work is to improve the properties of natural rubber composites (NRC) that were frequently used in medical and health supplies, using nanosilver additions. Silver nanocolloids were biosynthesized with an aqueous medium of aloe leaf extract (ALE) as capping agent, and then were filled in natural rubber matrix to prepare nanosilver-based NRC. UV–vis spectrophotometer, X-ray diffraction, and transmission electron microscopic analyses proved that the particle size of resultant silver was about 20 nm. The antibacterial activities against *Staphylococcus aureus* and *Escherichia coli* bacteria of NRC were dependable on the silver nanoparticles content and the treating methods on ALE, which was used in synthesizing silver nanocolloids. The morphology and thermal stability effect of nanosilver on NRC were determined with scanning electron microscopic and thermogravimetric analysis, respectively. © 2014 Wiley Periodicals, Inc. J. Appl. Polym. Sci. **2014**, *131*, 40746.

KEYWORDS: composites; morphology; nanoparticles; nanowires and nanocrystals; properties and characterization; rubber

Received 1 November 2013; accepted 18 March 2014
DOI: 10.1002/app.40746

INTRODUCTION

Biosynthesis of nanoparticles has been proposed as a cost-effective environmental friendly alternative to chemical and physical methods. Consequently, silver nanoparticles have been synthesized by using microorganisms and plant extracts.[1] Synthesis of nanoparticles using plant extracts is potentially advantageous over microorganism due to the ease of biohazards and the culture of the microorganism. Silver nanoparticles have been synthesized by using various plant extracts including hibiscus (*Hibiscus rosa sinensis*) leaf extract, neem (*Azadirachta indica*) leaf broth, black tea leaf extracts, Indian gooseberry (*Emblica officinalis*) fruit extract, sundried camphor (*Cinnamomum camphora*) leaves, and aloe leaf extract (ALE).[2,3] ALE is rich in chemical composition, such as glycoproteins, protein constituents, alkaloids, flavonoides, steroids, anthraquinones, and so forth.[4] S. Prathap Chandran has synthesized silver nanoparticles using Zingiber officinale extract which acts both as reducing and stabilizing agent, since Zingiber officinale holds amounts of alkaloids, flavonoides, steroids, anthraquinones, and so forth.[5,6] The overall observation proves the existence of some phenolic compounds, terpenoids or proteins that are bound to the surface of Ag nanoparticles that remained despite repeated washing. The stability of Ag nanoparticle may be due to the free amino and carboxylic groups that have interacted with the silver surface. The bonds of functional groups such as —CO—C—, —C—O—, and —C=C— are derived from heterocyclic compounds and the amide bands derived from the proteins are present in the leaf extract and are the capping ligands of the nanoparticle. Moreover, the proteins present in the medium prevent agglomeration and aid in the stabilization by forming a coat, covering the metal nanoparticles.[6]

The use of nanoparticles is gaining impetus in the present century, as they possess defined chemical, optical, and mechanical properties. The metallic nanoparticles are most promising as they show good antibacterial properties, which is coming up as the current interest in the researchers due to the growing microbial resistance against metal ions, antibiotics, and the development of resistant strains.[7] The current research supports that use of silver nanoparticles can be exploited in medicine for burn treatment, dental materials, coating stainless steel materials, textile fabrics, water treatment, sunscreen lotions, and so forth, and possess low toxicity to human cells, high thermal stability and low volatility.[8] In the studies of Feng et al.,[9,10] they suggested three main killing mechanisms for antibacterial properties of nanosilver. The first mechanism was nanosilver attached to the cell membrane and disturbing the permeability, respiration and other proper functions of the cell wall. The second mechanism they proposed was nanosilver penetrating through the cell wall and damaging the DNA of the bacteria. The third mechanism was silver ions released by nanosilver interacting with thiol groups in protein and inactivating the bacteria protein. In addition, these biosynthesized nanoparticles

Table I. Formulation of Latex Compound for the Synthesis of Antimicrobial Natural Rubber Latex Film Samples (phr)

Ingredients	Dry parts per hundred rubber (pphr)
61% Natural rubber latex concentrate	100
20% Potassium hydroxide	0.2
20% Peregal O (leveling agent O)	0.5
50% Sulfur	1
50% ZDC	1
40% Antioxidant (*N*-phenyl-2-naphthylamine)	1
40% ZnO	1
Silver nanoparticles	$X \times 3.23 \times 10^{-5}$ ($X = 0, 5, 10, 15, 20$)

might also be used as additives in water paints or cotton fabrics since there were previous reports on such nanoparticles displaying pronounced antimicrobial effects.[11]

The syntheses of antimicrobial composites with silver nanoparticles have been reported by many researchers. Li et al.[12] found that surgical masks coated with silver oxide nanoparticles do not cause skin allergy on the users. Maneerung et al. reported that the impregnation of freeze-dried silver nanoparticles into bacterial cellulose showed good antimicrobial activity against Gram-negative *Escherichia coli* (*E. coli*) and Gram-positive *Staphylococcus aureus* (*S. aureus*).[13] Roe et al. have found a method of making antimicrobial plastic catheters by silver nanoparticles on standard PE-BAX polyamide 20 gauge catheters.[14] Son et al. reported that the antimicrobial polymer nanofiber (cellulose acetate) can be synthesized by treating nanosilver on the surface by UV irradiation.[15]

On the basis of the available literature, we have synthesized silver nanoparticles by a biochemical method with silver nitrate as raw material, and ALE as capping agents; [16] made an attempt to find the best way to extract the aqueous ALE such as "ultrasonic cleaner," ultrasonic cell crushing apparatus and microwave. Furthermore, we investigated the antimicrobial effects of nanosilver on NRC against representative microorganisms of public concern, and also the mechanical and thermal properties of the NRC.

EXPERIMENTAL

Raw Materials

Chemicals for synthesis of silver nanoparticles were obtained from Guangzhou Pharmaceutical Holdings Limited, China. Natural rubber latex concentrate and other rubber chemicals for making NRC were supplied by Hainan Rubber Industry Group, China, and Sinopharm Chemical Reagent, China, respectively.

Synthesis of Nanosilver-Based NRC

Preparation of Aqueous Aloe Leaves Extract. Aloe leaves (50 g) were washed and extracted with 125 mL of distilled water at 40°C while being continuously treated for 20 min in the ultrasonic cleaner (setting parameters: frequency 40 Hz, power 240 W), microwave (power 200 W), and ultrasonic cell crushing apparatus (amplitude 50%, power 200 W), respectively. After extraction, samples were centrifuged at 3000 rpm for 5 min. The resultant supernatant was collected, filtered, decolorized with activated carbon, and stored at 0°C before use. This aqueous ALE, as the capping agent, was used for further experiments.[17,18]

Synthesis of Nanosilver. The silver nanoparticles used in this work were synthesized 15 days in advance according to the previously reported method by Zhang et al.[16] All experiments were carried out in triplicates and representative data were presented here. The formed nanoparticles were characterized further. The effect of ALE extracted with different methods was determined by varying the extracting methods [(A) ultrasonic cleaner, (B) ultrasonic cell crushing apparatus, (C) microwave].

Preparation of Nanosilver-Based NRC. The formulation used to make the natural rubber latex (NRL) compound was shown in Table I. First, the aqueous dispersions of sulfur, zinc diethyl dithiocarbamate (ZDC), antioxidant and zinc oxide (ZnO) were grinded for 12 h by the ball grinding mill, respectively. After 6 h, natural rubber latex concentrate was mixed with the aqueous dispersions, potassium hydroxide, "peregal O" and stirred at 20 rpm. After 0.5 h, previously prepared silver nanocolloids were slowly added to the mixture. Then, the NRL compound was matured for 4 h at room temperature with continuous stirring at 10 rpm.[19]

After maturation, the NRL compound was made into NRC by coating methods. The NRC was naturally dried (in room temperature) for about 5 days until the film was transparent, and the thickness of the NRC film was about 1.3 mm. Finally, the NRC film was vulcanized in a hot air oven (electric heater) at 100°C for 7 min. The same procedure was used to produce the control sample of NRC (without nanosilver).

Characterization of Nanosilver

The silver nanocolloidal sample was characterized with the help of a UV–vis spectrophotometer (TU-1901). The spectral background absorption was subtracted by using UV–vis spectra of aqueous ALE.

X-ray diffraction (XRD) data were taken with a Ni filter and Cu Kα radiation ($\lambda = 1.5406$ nm), on the D/MAX-IIIC powder diffractometer (Physics), operated in the θ: 2θ mode primarily in the 10°–80° (2θ) range and step-scan of $2\theta = 0.02°$. The tube voltage was 36 kV, and the tube current was 20 mA.

Transmission electron microscopic (TEM) measurements were performed on a JEOL TEM-2010 instrument (Japan) operated at an accelerating voltage of 200 kV, on which there is a CCD photo recorder. A drop of silver colloids was deposited on copper grid coated carbon membrane carefully by microsyringe for TEM and allowed the sample to dry at room temperature in a self-designed room for 1 h.

Characterization of Nanosilver-Based NRC

Determination of Antibacterial Activity. With the halo test method, the pathogenic strains of *E. coli* and *S. aureus* were used to determine the antibacterial activity of the

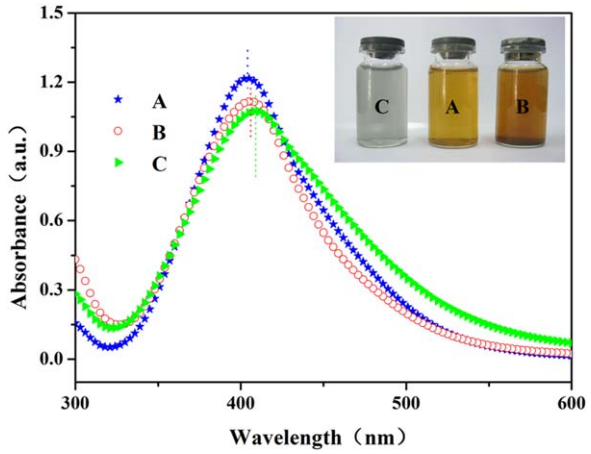

Figure 1. Visual observations and UV–vis absorption spectra of silver nanocolloids. Containing 1.0 mmol silver nitrate and 10.0 mL aqueous ALE extracted with different methods [(A) ultrasonic cleaner, (B) ultrasonic cell crushing apparatus, (C) microwave], incubated at room temperature for 20 min. [Color figure can be viewed in the online issue, which is available at wileyonlinelibrary.com.]

modified/unmodified natural rubber film materials. The bacterial cultures were maintained on Nutrient Agar (NA) slants. The test bacterial suspensions (100 μL) containing 10^4 cells mL^{-1} were spread on NA plates. Freshly prepared samples were cut into circles with the diameter being 5.5 mm ($\Phi O = 5.5$ mm), which would be put in the seeded plates. The samples were initially incubated for 15 min at 4°C (to allow diffusion) and later on at 37°C for 24 h for the bacterial cultures. Positive test results were scored when a halo of inhibition was observed around the NRC samples after the incubation.

Determination of Mechanical Properties. Dumbbell-shaped samples were cut from the molded sheets according to ASTM D-412. Tensile tests were carried out with a universal tensile machine XL-50A at a cross-head speed of 500 mm/min to determine the tensile properties in terms of tensile strength, stress at 100% elongation (S100), stress at 300% elongation (S300), and elongation at break. Tensile fractured samples were analyzed using Hitachi S-3000N scanning electron microscope (SEM). Tear strength was examined according to ASTM D-624 in unnecked 90° angular specimen using universal tensile machine XL-50A. The crosshead speed was 500 mm/min. ASTM Die-C was used for cutting samples.

Thermogravimetric Analysis. The thermogravimetric analysis (TGA) of NRC and nanosilver-based NRC vulcanizate was carried out by using a TG analyzer (SDT-Q600, America) in nitrogen (flow rate 50 mL/min) within the temperature range of 30–700°C. All these analyses were carried out at the heating rate of 10°C/min.

RESULTS AND DISCUSSION

UV–Vis Determination of Silver Nanocolloids

All of the reaction mixture of A, B, C (Figure 1) turned yellow-brown after 20 min of incubation, and then changed to the showed color in Figure 1. The color of the reaction mixtures changed with the extraction processing methods of ALE. As the ultrasonic cleaner method used, the best peak (position and shape) displayed, also the intensity was far higher than the others (Figure 1, tube A and curve A).[20–22] For the ultrasonic cell crushing apparatus extraction processing method of ALE, a dark brown color were observed (Figure 1, tube B), which likely related to the biomolecules partly damaged. The vibration frequency of the waves from ultrasonic cell crushing apparatus was stronger than the ultrasonic cleaner, so the bond of functional groups such as —CO—C—, —C—O—, —C=C—, and amide, which was derived from heterocyclic compounds and proteins in the leaf extract, might be damaged. [6] For the "microwave" method, lighter gray shade was obtained and the peak was proportionately less intense (Figure 1, tube C and curve C), which showed such biomolecules (ALE) were likely to be inactivated, since the temperature nearly came to 90°C (extremely condition) after the treatment by microwave. As the microwave method used, the resultant silver particles might be aggregated since the surface plasmon peak for silver nanoparticles trended to red-shift (Figure 1, curve C).[23]

XRD Analysis of Silver Nanoparticles

The XRD spectrum of silver nanoparticles was revealed in Figure 2 and the diffraction peaks at 2θ values of 38.42°, 44.53°, 64.59°, and 77.13° correspond to the crystal planes of (111), (200), (220), and (311), respectively, of a faced center cubic lattice of silver,[16] which were consistent with the earlier reports.[24] The average size of the silver nanoparticles was estimated as 20 nm using the Scherrer equation:

$$d = 0.9\lambda/\Delta(2\theta)\cos\theta,$$

where d is the crystalline domain size, $\Delta(2\theta)$ is the width at half-maximum of the strongest peak (111), and λ is the X-ray wavelength.

TEM Observation of Silver Nanoparticles

The TEM images of the silver nanoparticles in different extraction method were shown in Figure 3. As can be seen from the TEM images, the primary silver particles formed with ALE extracted by ultrasonic cleaner are nearly spherical nanoparticles with a diameter of approximately 20 nm [Figure 3(A)], which is consistent with the result of XRD analysis. The resultant silver particles of "microwave" were aggregated [Figure 3(C)], which

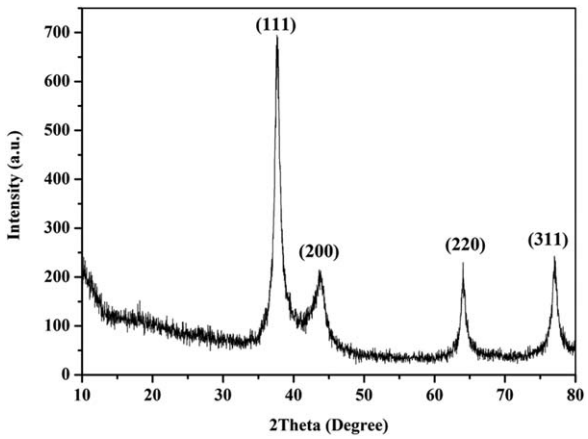

Figure 2. XRD profile of silver nanoparticle sample.

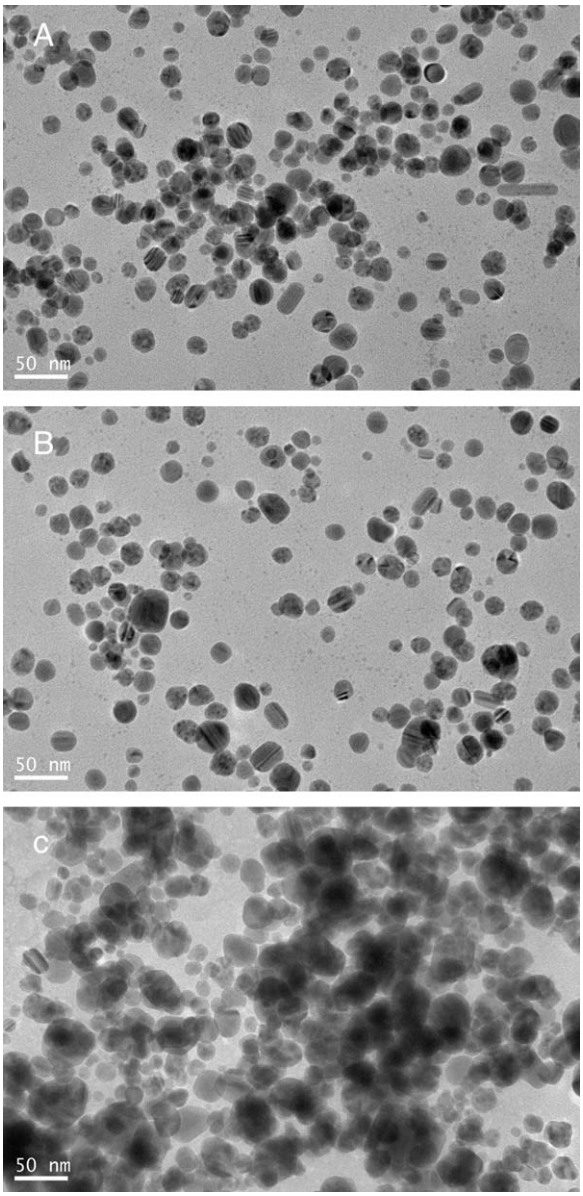

Figure 3. Transmission electron micrograph of silver nanoparticles synthesized with 10 mL aqueous ALE, 1.0 mmol silver nitrate and incubated at room temperature for 20 min [(A) ultrasonic cleaner, (B) ultrasonic cell crushing apparatus, (C) microwave].

agrees with the UV–vis determination (Figure 1, curve C). For the resultant silver particles of "ultrasonic cell crushing apparatus," it can be seen that the amount of silver particles [Figure 3(B)] was slightly less than that of ultrasonic cleaner [Figure 3(A)].

Antibacterial Properties of NRC

The silver nanoparticles incorporated aqueous ALE extracted have displayed antimicrobial activity towards the tested pathogenic strains of *E. coli* and *S. aureus*,[16] and the nanosilver-based NRC also displayed the same antimicrobial activity. In all the figures, the light zones around the round samples represented the inhibition zones. Figure 4(1) represented the inhibition zone observed from the samples against *E. coli* bacteria. The control NRC (containing ALE without nanosilver) displayed a little antimicrobial activity [Figure 4(1A)], which the actual reason was the microsized ZnO can also show antimicrobial activities.[25] In a similar manner, antibacterial activity was observed toward *S. aureus* [Figure 4(2)]. The antimicrobial activity (both types of bacterium) obtained with nanoparticles was comparable (Figure 5). It suggested that such nanosilver-based NRC was effective against both the tested bacteria *E. coli* and *S. aureus*, and it showed more significant antimicrobial activity against *S. aureus* than against *E. coli*.[26] The reason for the larger inhibition zone for *S. aureus* was the thicker cell wall contacting more peptidoglycan (PGN) layer in Gram-positive bacteria. According to the killing mechanism explained by Mirzajani et al.,[27] thicker PGN layer presents in Gram-positive bacteria can be easily damaged by silver nanoparticles. Another study reported that the positive charge on the silver ion is crucial for its antimicrobial activity through the electrostatic attraction between the negative charged cell membrane of the microorganism and positive charged nanoparticles.[28]

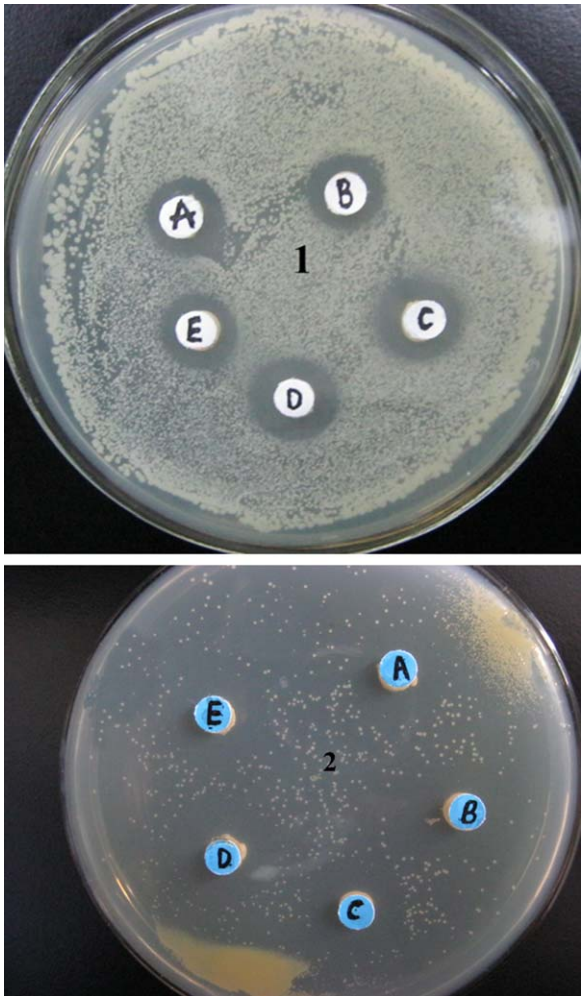

Figure 4. Antimicrobial activity against (1) *E. coli* and (2) *S. aureus* of nanosilver-based NRC containing 70.0 g NRC and different dosage of silver nanoparticles (g) [(A) 0, (B) 1.62×10^{-4}, (C) 3.23×10^{-4}, (D) 4.85×10^{-4}, (E) 6.46×10^{-4}]. [Color figure can be viewed in the online issue, which is available at wileyonlinelibrary.com.]

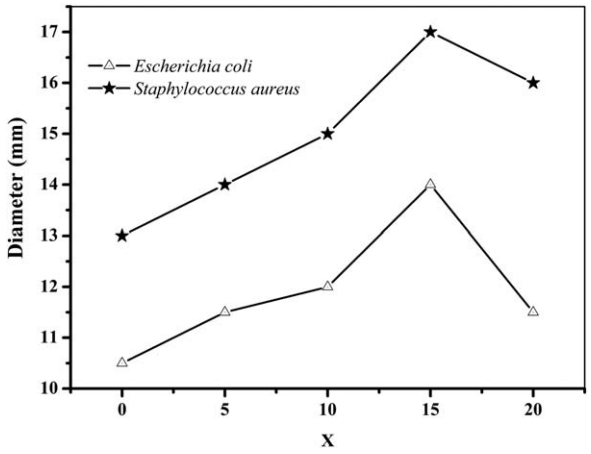

Figure 5. The average size of inhibition zone diameter with different dosage of silver nanoparticles (g) [$X \times 3.23 \times 10^{-5}$ ($X = 0, 5, 10, 15, 20$)]

Figure 5 indicated the more dosage of the nanosilver the more obvious antimicrobial activity against *E. coli* and *S. aureus*. But when the dosage was arrived at X = 20, the inhibition zones turned smaller, which might due to the aggregation of the silver nanoparticles leading to larger size.[29]

Figure 6 and Table II showed antimicrobial activity of NRC containing silver nanocolloids synthesized with different extraction processing methods on ALE. It was concluded that the single ALE (without nanosilver) displayed little antimicrobial activity and the NRC containing nanosilver synthesized with ultrasonic cleaner method on ALE showed the best antimicrobial activity.[27] It was in agreement with the earlier results of UV–vis and TEM analysis, as the better peak (position and shape) displayed and the smaller particles with the ultrasonic cleaner extraction processing method on ALE.

Morphology of NRC

The SEM pictures of fractured surfaces of tensile specimen of NRC samples were shown in Figures 7 and 8. All the fracture surfaces of the NRC were rough and showed the extended deformation before failure. It can be seen that there were large amount of pinholes or physical voids on the surface of control NRC [Figure 7(A)], but the tensile fracture surfaces of composites containing silver nanoparticles [from 1.62×10^{-4} to 4.85×10^{-4} g; Figure 7(B–D)] were relatively smoother. It might be that the organic biomolecules (ALE) around silver nanoparticles had good compatibility with the natural rubber matrix, which made nanaoparticles work as a kind of reinforcing filler resulting in the improvement of the mechanical properties. Figure 7(E) revealed that the fracture surface changed rougher with the further increment of silver nanoparticles.[28]

Fewer pinholes or physical voids were observed on the surface of Figure 8(B–D) than Figure 8(A), and we might conclude the single ALE cannot enhance the mechanical properties of NRC as much as silver nanoparticles. However, more pinholes or physical voids were seen on the fractured surface on Figure 8(D), which might reduce the tensile strength of the NRC.[31–33] In conclusion, the ALE extracted by ultrasonic cleaner played better role in protecting the formed silver nanoparticles in the NRC.

Mechanical Properties of NRC

Table III showed the effect of silver nanoparticles content on mechanical properties of NRC. The tensile strength of control NRC was 22.42 MPa and developed with the increasing addition of silver nanoparticles (from 0 to 3.23×10^{-4} g) up to 24.01 MPa and reduced to 23.82 MPa (6.46×10^{-4} g). Modulus of NRC at 100%, 300% elongation, and elongation at break changed little when the nanosilver was added. At the same time, the tear strength increased with the increased nanosilver content (from 0 to 3.23×10^{-4} g) in a dose-dependent manner, since it perhaps that nanoparticles acted as crosslinking points creating higher crosslink density of rubber vulcanizates.[32] As crosslink density increased with the increasing silver nanoparticles content in the rubber matrix, the chain mobility decreased and more loading was required for tear strength, which might also

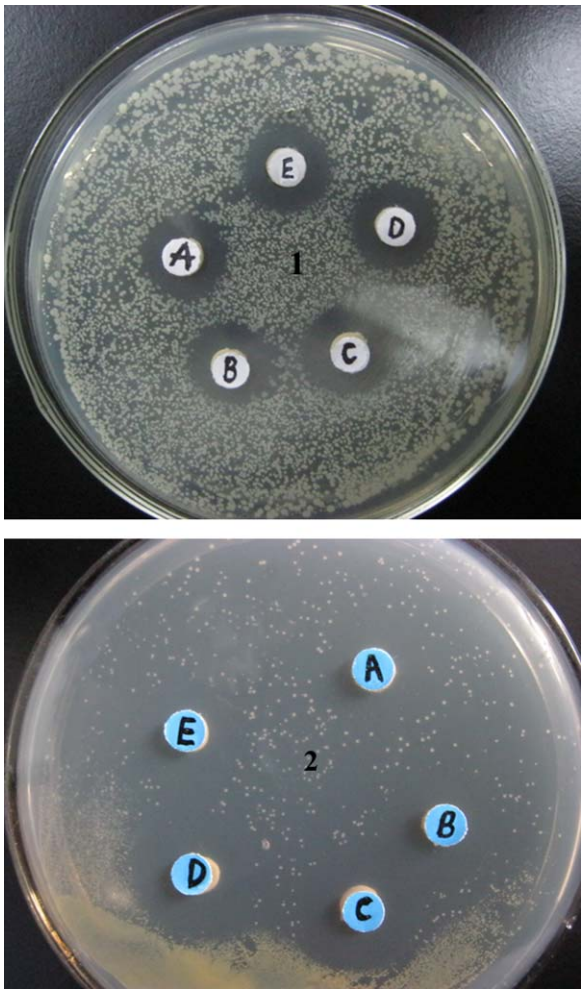

Figure 6. Antimicrobial activity against (1) *E. coli* and (2) *S. aureus* of NRC containing silver nanoparticles (4.85×10^{-4} g) formed by ALE with different extraction processing methods [(A) control (containing ALE without nanosilver), (B) microwave, (C) ultrasonic cleaner, (D) ultrasonic cell crushing apparatus, (E) positive control (gentamycin •400 units/mL)]. [Color figure can be viewed in the online issue, which is available at wileyonlinelibrary.com.]

Table II. Size of Inhibition Zone Diameter with Different Extraction Processing Methods

		Size of inhibition zone diameter (mm)	
Item	Extraction processing methods	*E. coli*	*S. aureus*
a	Control (containing ALE without nanosilver)	13.0	13.0
b	Microwave	14.0	15.0
c	Ultrasonic cleaner	15.0	17.0
d	Ultrasonic cell crushing apparatus	14.5	16.0
e	Positive control	15.5	15.0

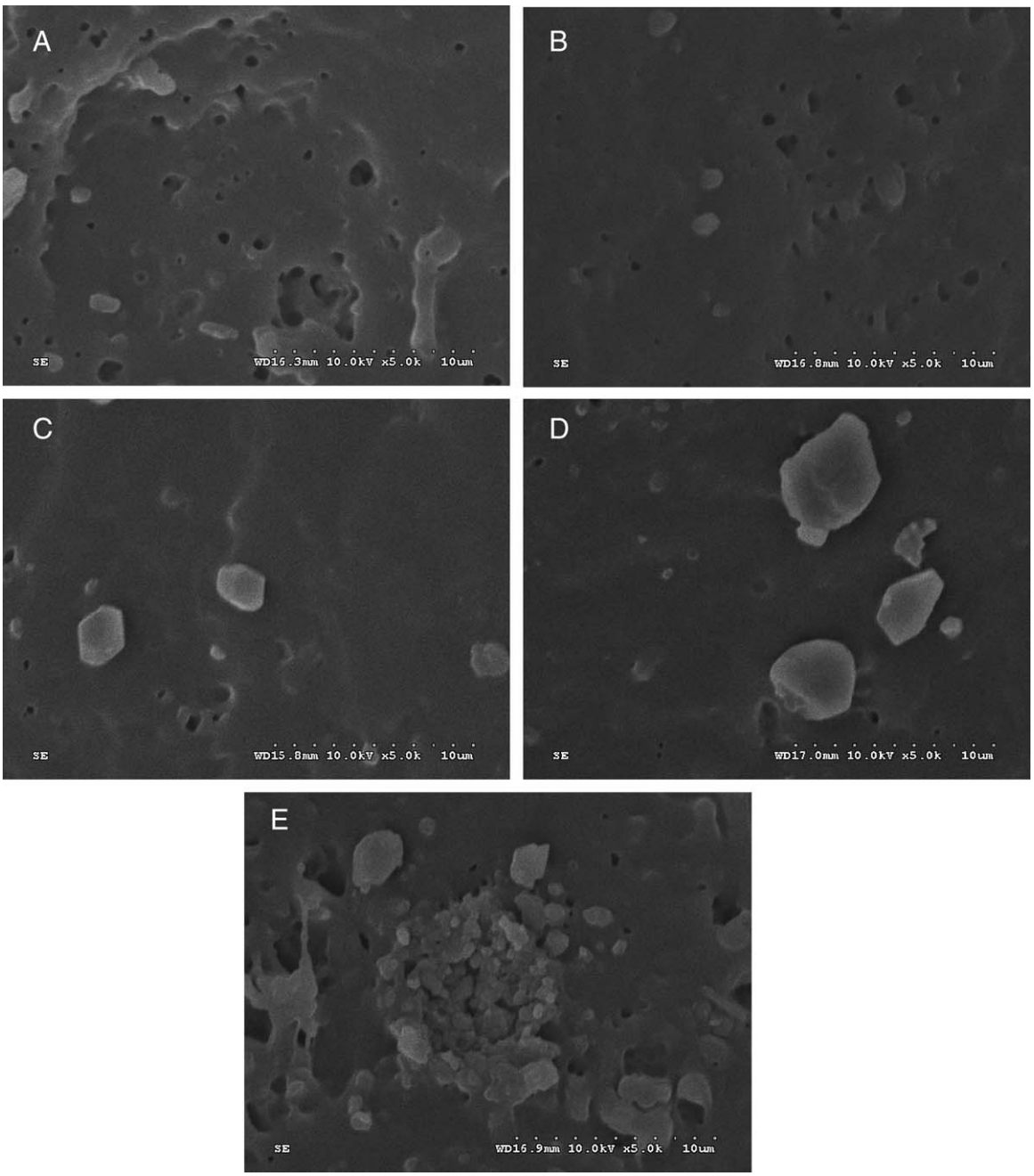

Figure 7. SEM pictures of tensile fracture surfaces: (WD 16.0 mm 10.0 kV × 5k) containing 70.0 g NRC and different dosage of silver nanoparticles (g) [(A) 0, (B) 1.62×10^{-4}, (C) 3.23×10^{-4}, (D) 4.85×10^{-4}, (E) 6.46×10^{-4}].

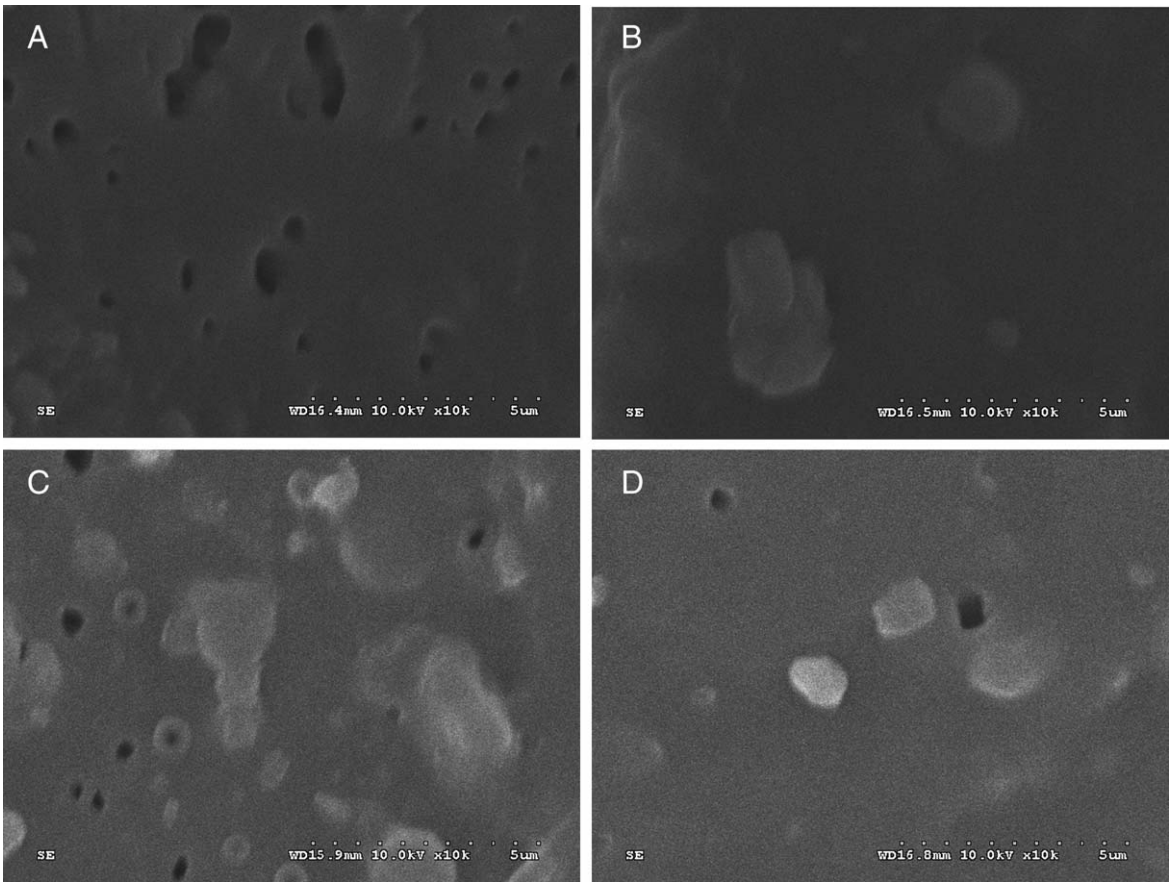

Figure 8. SEM pictures of tensile fracture surfaces: (WD 16.0 mm 10.0 kV × 10k) containing silver nanoparticles (3.23×10^{-4} g) with different treating methods on ALE: [(A) control (containing ALE without nanosilver), (B) ultrasonic cleaner, (C) ultrasonic cell crushing apparatus, (D) microwave].

be explained on the basis of nanoparticles worked as a kind of effective reinforcing filler.[34] But it decreased slightly upon the increment of nanosilver content ($X \geq 15$), which might be the silver nanoparticles tended to aggregate and were difficult to disperse in the NRC.[6]

The effect of the ALE extraction processing methods on the mechanical properties was shown in Table IV. The tensile strength and tear strength of the NRC both transformed with the varing extraction methods on ALE, while the others remained essentially the same or decreased slightly. It suggested that the silver nanocolloids synthesized with ultrasonic cleaner method preferred to reinforce the mechanical properties of NRC. This was consistent with the previous results from Figure 1 that the formed nanaoparticles were in best dispersion and less size with ultrasonic cleaner method. Under the extremely extraction conditions (microwave and ultrasonic cell crushing apparatus), such biomolecules (some compounds of the aloe are containing a large number of hydroxyl and carbonyl groups in aqueous solution) were likely to be inactivated.[35] Also the cause for higher tensile strength and tear strength had also been analyzed by conducting the fractography studies of tensile fracture surface using SEM in the above.

Thermogravimetric Analysis of NRC

Thermal degradation of NRC vulcanizates in nitrogen atmosphere was analyzed and the corresponding results were given in Figure 9. Figure 9(A) showed the TGA curves of control NRC

Table III. Mechanical Properties of NRC Containing Different Dosage of Silver Nanoparticles

	Silver nanoparticles (g)				
Item	0	1.62×10^{-4}	3.23×10^{-4}	4.85×10^{-4}	6.46×10^{-4}
Tensile strength (MPa)	22.42	22.75	24.01	23.81	23.82
Tear strength (kN/m)	34.65	37.29	42.19	37.83	35.33
S100 (MPa)	0.65	0.66	0.69	0.65	0.67
S300 (MPa)	1.20	1.21	1.34	1.20	1.21
Elongation at break (%)	870	870	860	830	850

Table IV. Mechanical Properties of NRC Containing Silver Nanoparticles (3.23×10^{-4} g) with Different Treating Methods on ALE

	Extraction processing method			
Item	Control (containing ALE without nanosilver)	Ultrasonic cleaner	Ultrasonic cell crushing apparatus	Microwave
Tensile strength (MPa)	20.44	23.49	23.44	23.07
Tear strength (kN/m)	30.62	52.32	33.40	32.24
S100 (MPa)	0.55	0.58	0.61	0.57
S300 (MPa)	1.01	0.99	1.11	1.04
Elongation at break (%)	910	990	870	930

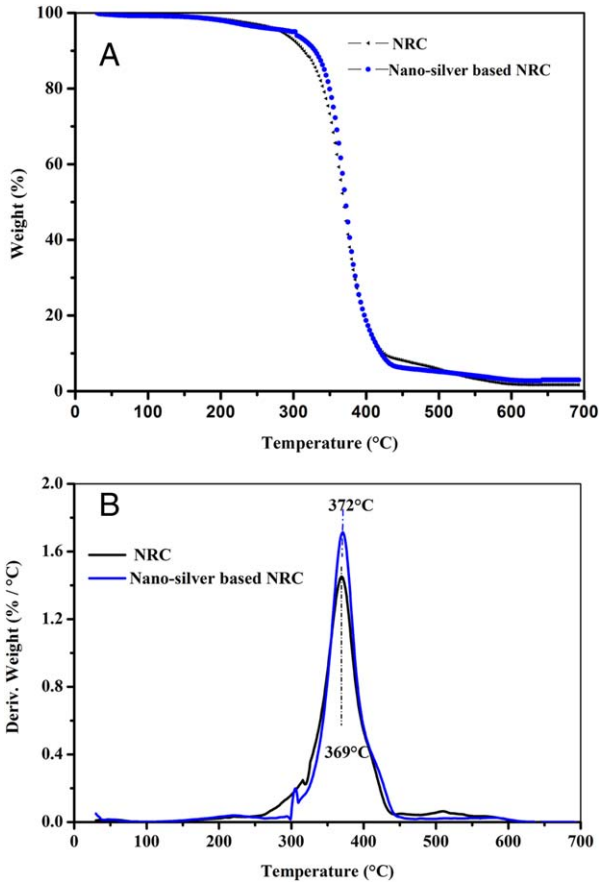

Figure 9. TGA/DTG curves of NRC and nanosilver-based NRC. [Color figure can be viewed in the online issue, which is available at wileyonlinelibrary.com.]

and nanosilver-based NRC from 30 to 700°C. It showed that mass loss of NRC and at the same time nanosilver-based NRC varied significantly. Nanosilver-filled composites revealed enhanced thermal barrier against mass loss. The mass loss of control NRC over the temperature range was higher than that of nanosilver-filled NRC. Table V suggested the weight loss of materials at various temperatures. The 5% weight loss for control NRC was observed at 287.5°C and nanosilver-based NRC (filled with 3.23×10^{-4} g silver nanoparticles) was at higher temperature of 304.5°C.

Moreover, Table V displayed the weight retention percent of composites at different temperatures. Weight loss due to moisture was found at around 110°C in the composite specimens. NRC showed more weight loss than that of nanosilver-filled composites due to moisture evaporation. It was likely to be that the more nanosilver content in the rubber, the less weight loss due to moisture; and the rubber material usually contains more content of moisture.[32] It was observed that up to 300°C, the weight loss was within 10% and in range of 300–400°C the weight loss was severer. The table further revealed that at the majority of given temperatures (except 200 and 500°C), the mass loss was higher in NRC than that of nanosilver-filled. The DTG curves [Figure 9(B)] revealed that the maximum degradation rate of NRC appeared at 369°C, which was lower than the nanosilver-based NRC' 372°C.[36] From both the TGA and DTG curves, it was clear the nanosilver-based NRC was likely to show superior aging resistance property than the control NRC.

CONCLUSIONS

In this study, we have used an agricultural plant material for the homogeneity and quick synthesis of nanosilver-based NRC. Typical colors and UV–visible spectra revealed that the compounds extracted from ALE played a good capping role in synthesizing silver nanoparticles. High-quality silver nanoparticles (20 nm) were obtained availably when the ALE was extracted by ultrasonic cleaner. The antibacterial activities of the resultant NRC samples toward the tested bacterial cultures (*E. coli* and *S. aureus*) were enhanced by the biosynthesized nanosilver,

Table V. TGA Properties of NRC and Nanosilver-Based NRC

		% Weight retention at						
Material	Temp at 5% weight loss (°C)	110°C	150°C	200°C	300°C	400°C	500°C	600°C
Control NRC	287.5	99.12	98.87	98.89	92.95	18.39	5.94	1.84
Nanosilver-based NRC	304.5	99.69	99.31	97.82	95.05	18.59	5.09	3.34

especially formed by the ultrasonic cleaner method on ALE. Tensile strength and tear strength were improved with the increment of silver nanoparticles in a certain range ($X = 0$–10) and then decreased, while modulus and elongation at break of NRC changed little. It was observed from SEM that tensile fracture surfaces of NRC with silver nanoparticles (from 1.62×10^{-4} to 4.85×10^{-4} g) were relatively smoother (fewer pinholes or physical voids) than the others. TGA results revealed the thermal stability of NRC was enhanced with the biosynthesized nanosilver obviously. In conclusion, the loading NRC with nanosilver could be used as antibacterial and reinforced natural rubber composites. These in turn, could be applied in the fields of pacifiers, medical gloves, ureter, blood bags, and other medical and health supplies.

ACKNOWLEDGMENTS

This work was financially supported by National Natural Science Foundation (grant no. 21264006), China; and Hainan Provincial Natural Science Foundation (grant no. 509002).

AUTHORS' CONTRIBUTION

Y.Z. wrote the paper and X.X. revised it critically. X.X. and G.L. conceived and directed the research. Y.Z., Z.Z., and Y.L. prepared the samples and carried out characterization.

REFERENCES

1. Sun, D. H.; Li, Q. B.; He, N.; Huang, J. L.; Wang, H. X. *Rare Metal Mat. Eng.* **2011**, *40*, 148.
2. Njagi, E. C.; Huang, H.; Stafford, L.; Genuino, H.; Galindo, H. M.; Collins, J. B.; Hoag, G. E.; Suib, S. L. *Langmuir* **2011**, *27*, 264.
3. Huang, X. C.; Lin, H.; Chen, Y. Y. *J. Silk (China)* **2009**, *10*, 26.
4. Ojha, N. K.; Kumar, A. *Asian Pac. J. Trop. Dis.* **2012**, *2*, 104.
5. Sangeetha, G.; Rajeshwari, S.; Venckatesh, R. *Mater. Res. Bull.* **2011**, *46*, 2560.
6. Chandran, S. P.; Chaudhary, M.; Pasricha, R.; Ahmad, A.; Sastry, M. *Biotechnol. Prog.* **2006**, *22*, 577.
7. Gong, P.; Li, H. M.; He, X. X.; Wang, K. M.; Hu, J. B.; Tan, W. H.; Zhang, S. C.; Yang, X. H. *Nanotechnology* **2007**, *18*, 604.
8. Duran, N.; Marcarto, P. D.; De Souza, G. I. H.; Alves, O. L.; Esposito, E. *J. Biomed. Nanotechnology* **2007**, *3*, 203.
9. Morones, J. R.; Elechiguerra, J. L.; Camacho, A.; Holt, K.; Kouri, J. B.; Ramirez, J. T.; Yacaman, M. *J. Nanotechnology* **2005**, *16*, 2346.
10. Feng, Q. L.; Wu, J.; Chen, G. Q.; Cui, F. Z.; Kim, T. N.; Kim, J. O. *J. Biomed. Mater. Res.* **2000**, *52*, 662.
11. Khaydarov, R. R.; Khaydarov, R. A.; Evgrafova, S.; Wagner, S.; Cho, S. Y. In Environmental Security and Ecoterrorism (NATO Science for Peace and Security Series C: Environmental Security) Springer Netherlands: Netherlands, **2011**, Chapter *9*, p 117.
12. Li, Y.; Leung, P.; Yao, L.; Song, Q.; Newton, E. *J. Hosp. Infect.* **2006**, *62*, 58.
13. Maneerung, T.; Tokura, S.; Rujiravanit, R. *Carbohydr. Polym.* **2008**, *72*, 43.
14. Roe, D.; Karandikar, B.; Bonn-Savage, N.; Gibbins, B.; Roullet, J. B. *J. Antimicrob. Chemother.* **2008**, *61*, 869.
15. Son, W. K.; Youk, J. H.; Park, W. H. *Carbohydr. Polym.* **2006**, *65*, 430.
16. Zhang, Y. Q.; Cheng, X. F.; Zhang, Y. C.; Xue, X. H.; Fu, Y. Z. *Colloids Surf. A Physicochem. Eng. Asp.* **2013**, *423*, 63.
17. Long, M. H.; Zhang, G. Q.; Zhang, C. X. *J. Anhui Agric. Sci.(China)* **2011**, *39*, 7081.
18. Dwivedi, A. D.; Gopal, K. *Colloids Surf. A Physicochem. Eng. Asp.* **2010**, *369*, 27.
19. Gu, J. C.; Tan, H. S.; He, Y. P.; Liao, X. X.; Li, J. G.; Jia, Y. G. *Special Purpose Rubber Products (China)* **2012**, *33*, 9.
20. Bankar, A.; Joshi, B.; Kumar, A. R.; Zinjarde, S. *Colloids Surf. A Physicochem. Eng. Asp.* **2010**, *368*, 58.
21. Pimprikar, P. S.; Joshi, S. S.; Kumar, A. R.; Zinjarde, S. S.; Kulkarni, S. K. *Colloids Surf. B Biointerfaces* **2009**, *74*, 309.
22. Mulvaney, P. *Langmuir* **1996**, *12*, 788.
23. Balan, L.; Malval, J. P.; Schneider, R.; Burget, D. *Mater. Chem. Phys.* **2007**, *104*, 417.
24. Sathishkumar, M.; Sneha, K.; Won, S. W.; Cho, C. W.; Kim, S.; Yun, Y. S. *Colloids Surf. B Biointerfaces* **2009**, *73*, 332.
25. Yamamoto, O. *Int. J. Inorgan. Mater.* **2001**, *3*, 643.
26. Eby, D. M.; Scheaeublin, N. M.; Farrington, K. E.; Hussain, S. M.; Johnson, G. R. *ACS Nano* **2009**, *3*, 984.
27. Mirzajani, F.; Ghassempour, A.; Aliahmadi, A.; Esmaeili, M. A. *Res. Microbiol.* **2011**, *162*, 542.
28. Hamouda, T.; Myc, A.; Donovan, B.; Shih, A. Y.; Reuter, J. D.; Baker, J. R. *Microbiol. Res.* **2001**, *156*, 1.
29. Rathnayake, W. G. I. U.; Ismaila, H.; Baharin, A.; Darsanasiri, A. G. N. D.; Rajapakse, S. *Polym. Test.* **2012**, *31*, 586.
30. Wang, Z. F.; Lin, H.; Zhang, K. X.; Wang, J.; Fu, X. *China Elastomerics* **2008**, *18*, 26.
31. Mohan, T. P.; Kuriakose, J.; Kanny, K. *J. Ind. Eng. Chem.* **2011**, *17*, 264.
32. De, D.; Pandab, P. K.; Royc, M.; Bhuniad, S. *Mater. Design* **2013**, *46*, 142.
33. Fu, J. F.; Yu, W. Q.; Dong, X.; Chen, L. Y.; Jia, H. S.; Shi, L. Y.; Zhong, Q. D.; Deng, W. *Mater. Design* **2013**, *49*, 336.
34. Prasertsri, S.; Rattanasom, N. *Polym. Test.* **2012**, *31*, 593.
35. Phumying, S.; Labuayai, S.; Swatsitang, E.; Amornkitbamrung, V.; Maensiri, S. *Mater. Res. Bull.* **2013**, *48*, 2060.
36. Lee, Y. S.; Lee, W. K.; Cho, S. G.; Kim, I.; Ha, C. S. *J. Anal. Appl. Pyrolysis* **2007**, *78*, 85.